hydrated form, resulting in negative $\bar{C}_{p2}$ values. Because there are a finite number of hydrogen bonds present in water, the extent to which hydrogen bonding is affected, and thus the negative contributions, decreases with increasing concentrations. When the positive contribution to the heat capacity from the hydrated ionic species exceeds the negative contribution, $\bar{C}_{p2}$ values become positive.

The radii of the trivalent rare earth ions are known to decrease monotonically from La to Lu; therefore, the charge density at the surface of the ions increases across the rare earth series. This higher charge density would exert a greater influence on the hydrogen bonding of water, and one might expect that $\bar{C}_{p1}$ would decrease across the rare earth series with decreasing ionic radii. As evident from Figure 6, $\bar{C}_{p1}$ values for dilute rare earth perchlorate solutions do not follow a monotonic trend across the rare earth series but rather illustrate the two-series effect owing to the change in inner sphere coordination plus resulting changes in outer spheres. It is interesting that the two-series effect is evident over the whole concentration range, although it does appear in Figure 4 that at high concentrations the break points in the curve shift to higher atomic numbers. It should be recalled however, that unlike the dilute solution where the outer spheres consist mainly of water molecules, in the concentrated solutions the outer spheres are made up mostly of outer sphere complexes with the perchlorate ion.

As illustrated in Figure 1, above 2.5 m, ϕ_{cp} for the lighter rare earths through Gd increases almost linearly with molality, whereas for the heavier rare earths, deviation from linear behavior is greater. At high concentrations this results in an increased separation in the $\bar{C}_{p1}$ curves of Figure 3 and in a distinct difference in the shape of the $\bar{C}_{p2}$ vs. m curves of Figure 2 for the heavy rare earths relative to the light.

Literature Cited

(1) Derer, J. L., unpublished PhD thesis, Iowa State University, Ames, Iowa, 1974.
(2) Epiken, Y. A., Stakhanova, M. S., *Zh. Fiz. Khim.*, **41**, 2148 (1967).
(3) Jekel, E. C., Criss, C. M., Cobble, J. W., *J. Amer. Chem. Soc.*, **86**, 5404 (1964).
(4) Mohs, M. A., unpublished PhD thesis, Iowa State University, Ames, Iowa, 1970.
(5) Osborne, N. S., Stimson, H. F., Ginnings, D. C., *J. Res. Nat. Bur. Stand.*, **23**, 197 (1939).
(6) Randall, M., Rossini, F. D., *J. Amer. Chem. Soc.*, **51**, 323 (1929).
(7) Spedding, F. H., Csejka, D. A., DeKock, C. W., *J. Phys. Chem.*, **70**, 2423 (1966).
(8) Spedding, F. H., Cullen, P. F., Habenschuss, A., *ibid.*, **78**, 1106 (1974).
(9) Spedding, F. H., Jones, K. C., *ibid.*, **70**, 2450 (1966).
(10) Spedding, F. H., Miller, C. F., *J. Amer. Chem. Soc.*, **74**, 3158 (1952).
(11) Spedding, F. H., Pickal, M. J., Ayers, B. O., *J. Phys. Chem.*, **70**, 2440 (1966).
(12) Spedding, F. H., Saeger, V. W., Gray, K. A., Boneau, P. K., Brown, M. A., DeKock, C. W., Baker, J. L., Shiers, L. E., Weber, H. O., Habenschuss, A., *J. Chem. Eng. Data*, **20** (1), 72 (1975).
(13) Spedding, F. H., Shiers, L. E., Brown, M. A., Derer, J. L., Swanson, D. L., Habenschuss, A., *ibid.*, p 81.
(14) Templeton, D. H., Dauben, C. H., *J. Amer. Chem. Soc.*, **76**, 5237 (1954).

Received for review October 29, 1974. Accepted January 4, 1975. Paper based on theses submitted by J. L. B. and J. P. W. in partial fulfillment for the PhD degree at Iowa State University. Report numbers IS-T-491 and IS-1988.

Adsorption of Hydrocarbons on Carbon Molecular Sieve—Application of Volume Filling Theory

Tomoko Nakahara,[1] Mitsuho Hirata, and Toshiaki Ohmori
Department of Industrial Chemistry, Tokyo Metropolitan University, Tokyo, Japan

Adsorption data of methane, ethylene, ethane, propylene, and propane on a microporous carbon molecular sieve were examined by Dubinin's volume filling theory. The Dubinin-Astakhov three-parameter characteristic equation $W = W^\circ \exp\{-(A/E)^n\}$ (where W is the pore volume, W° is the total pore volume, A is the adsorption potential, E is the characteristic energy, and n is the integer constant), was applied to data reduction. The adsorption data were well characterized by the equation for $n = 3$. The total pore volume and the characteristic energy were obtained. The generalized characteristic curve for hydrocarbons was obtained by using an affinity coefficient. Isosteric heat, differential heat of adsorption at constant coverage, and distribution of adsorption potential were calculated. The effect of microporosity of the adsorbent is discussed and compared with reported data for charcoal.

This work is the second part of a continuing study of adsorption of gases and vapors on microporous adsorbent. In the previous paper (*7*), the experimental adsorption data were reported for hydrocarbons on commercial-grade carbon molecular sieve designated as Molecular Sieving Carbon-5A (MSC-5A) by Takeda Chemical Ind. Co. It has micropores of approximately 5 Å in diameter, and its physical properties were described in the previous paper (*7*). The reported experimental adsorption isotherms were for pure adsorbates methane and benzene at 5.4° and 30.0°C; ethylene, propylene, and propane at 5.4°, 30.0°, and 50.0°C; *n*-butane at 5.4°, 30.0°, and 51°C; and *n*-pentane and cyclohexane at 30.0°C, all at pressures up to 650 mm Hg.

[1] To whom correspondence should be addressed.

Volume Filling Theory and Experimental Data Analysis

The adsorption force-field ranges over the inside of the entire volume of micropores for adsorbents such as MSC-5A. Therefore, adsorption of vapor in micropores leads to the volume filling rather than the layer-by-layer filling of micropore surface. The conception of volume filling theory developed by Dubinin (*3*) was in principle based on Polanyi's potential theory (*8*). The force of attraction at any given point in the adsorbed film is conveniently measured by the adsorption potential A, defined as the work done by the adsorption force in bringing a

molecule from the gas phase to that point. The process of building up the adsorbed film may therefore be represented by a function between W and A, $A = f(W)$, which is in reality a distribution function. The adsorbed potential is expressed as Equation 1 by putting a normal liquid state at equilibrium temperature as a standard state, and the filled volume W is defined by the liquefied adsorbate volume per gram of adsorbent:

$$A = RT \ln (P_s/P)$$
$$W = av/M \tag{1}$$

where a is the adsorption amount, v is the liquid molar volume, and M is the molecular weight. The distribution function between A and W may be expressed by Dubinin (*1*) as Equation 2:

$$\theta = \frac{W}{W^\circ} = \exp\left\{-\left(\frac{A}{E}\right)^n\right\} \tag{2}$$

where θ is the adsorption ratio, E is the characteristic energy, W° is the total pore volume, and n is the constant 1, 2, or 3. It is reported by Kawazoe et al. (*5*) that n should be 1 for the nonporous surface, 2 for the macroporous and transitional porous adsorbent (Equation 2 then becomes a Gaussian distribution), and 3 for the microporous adsorbent.

To generalize various gases and vapors on the same adsorbent, Dubinin introduced the affinity coefficient $\beta = E/E_o$ as a shifting factor into Equation 2, where E_o is a characteristic energy of a standard adsorbate. The value of β was nearly equal to the liquid volume ratio v/v_o.

$$W = W^\circ \exp\left\{-\left(\frac{1}{E_o}\cdot\frac{A}{\beta}\right)^n\right\} \tag{2a}$$

Although the volume filling theory was developed for vapor adsorbates, it may be applied to gases to some extent by assuming the hypothetical liquid volume and hypothetical saturated vapor pressure obtained by extrapolation into a supercritical region. The liquefied adsorbate volume for obtaining W is calculated by three ways depending on equilibrium temperatures.

Case 1. For vapors ($T_b > T$, where T and T_b are the equilibrium and normal boiling temperatures, respectively), v is the liquid molar volume at saturation pressure and is calculated by the method of the Technical Data Book (*9*).

Case 2. For vapors ($T_c > T \geq T_b$, where T_c is the critical temperature), v is obtained by the Dubinin-Nikolaev method (*2*) of Equation 3:

$$\rho^* = \rho_b - \frac{\rho_b - \rho_c}{T_c - T_b}(T - T_b)$$
$$\rho_c = \frac{M}{b},\ b = \frac{RT_c}{8P_c} \tag{3}$$

where ρ^* is the adsorbed phase density, ρ_b and ρ_c are the densities at normal boiling point and at critical temperature, respectively, and b is the van der Waals constant.

Case 3. For gases ($T \geq T_c$), v is the hypothetical liquid volume obtained by extrapolation of Equation 3 into a supercritical region. The hypothetical vapor pressure for Equation 1 is calculated by Equation 4.

$$P_s = P_c \exp\left(\frac{T - T_c}{T}\cdot\frac{\Delta H}{RT_c}\right) \tag{4}$$

Heat of adsorption may be calculated in analogy with the Clausius-Clapeyron equation for the heat of vaporization. Combining Equations 1 and 2 and differentiating ln (P_s/P) with respect to reciprocal temperature at constant θ, Equation 5 is obtained:

$$\left(\frac{\partial \ln (P_s/P)}{\partial (1/T)}\right)_\theta = \frac{E}{R}\left[\ln\left(\frac{1}{\theta}\right)\right]^{\frac{1}{n}} \tag{5}$$

The heat of adsorption at constant θ is defined as q_θ by Equation 6:

$$\left(\frac{\partial \ln P}{\partial (1/T)}\right)_\theta = -\frac{q_\theta}{R} \tag{6}$$

Substituting Equation 6 and the Clausius-Clapeyron equation into Equation 5, q_θ is expressed by Equation 7:

$$q_\theta = \Delta H + E\left(\ln\frac{1}{\theta}\right)^{\frac{1}{n}} \tag{7}$$

The isosteric heat of adsorption can be calculated from experimental data.

According to Polanyi's potential theory, the pore volume W is the adsorption space where the adsorption potential above A works. Adsorption in the adsorption space takes place successively from a higher potential space to the lower. Therefore, the derivative dW/dA is a distribution of adsorption potential. The following equation is obtained by differentiating Equation 2 with respect to A and by normalization:

$$-\frac{1}{W^\circ}\frac{dW}{dA} = n\frac{A^{n-1}}{E^n}\exp\left[-\left(\frac{A}{E}\right)^n\right] \tag{8}$$

The left-hand side of Equation 8 represents a probability distribution of the potential.

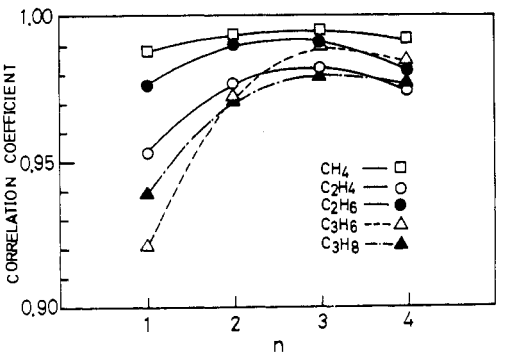

Figure 1. Correlation coefficient as function of exponent n in Equation 2

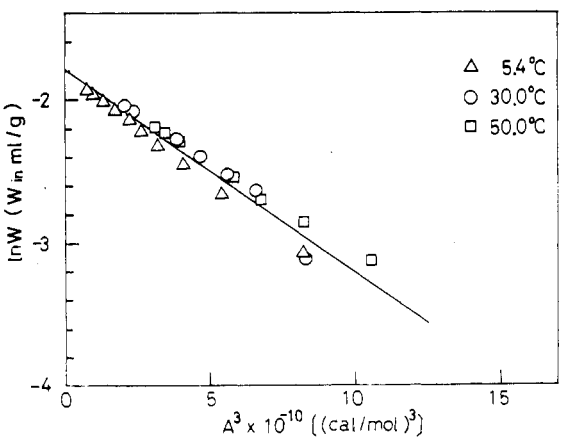

Figure 2. Characteristic curve for ethylene at $n = 3$

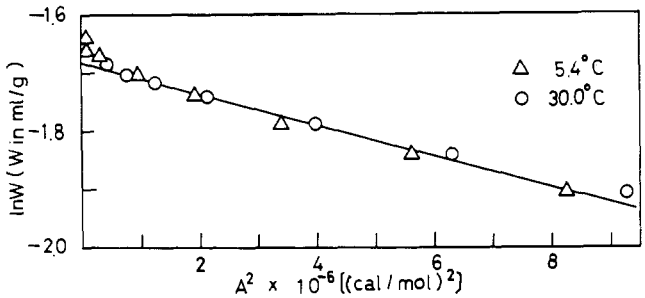

Figure 3. Characteristic curve for *n*-butane at $n = 2$

Table I. Calculated Parameters of Characteristic Equation (Equation 2) for Hydrocarbon-MSC-5A Systems and Heat of Vaporization for Hydrocarbons

Adsorbate	Total pore vol W°, ml/g-adsorbent	Characteristic energy E, kcal/mol	Heat of vaporization ΔH, kcal/mol[a] (temp range, °C)
Methane	0.125	3.51	2.13 (−205.9 ∼ −82.3)
Ethylene	0.167 (0.175)[b]	4.12 (3.80)[b]	3.27 (−168.3 ∼ +8.9)
Ethane	0.165 (0.162)[b]	4.13 (3.75)[b]	3.51 (−159.5 ∼ +23.6)
Propylene	0.184	4.83	4.70 (−131.9 ∼ +85.0)
Propane	0.165	4.62	4.81 (−128.9 ∼ +94.8)

[a] From ref. 4. [b] From ref. 5.

Table II. Affinity Coefficient and Liquid Molar Volume at 30°C

Ethane is standard substance

Adsorbate	Affinity coefficient β E/E_o	v/v_o	v, ml/mol
Methane	0.78	0.85	50.5[a]
Ethylene	0.93	1.00	64.8[a]
Ethane	1.00	1.00	60.0[a]
Propylene	1.17	1.14	82.8
Propane	1.28	1.12	75.6

[a] Extrapolated values.

Results and Discussion

The experimental data for adsorption of hydrocarbons on MSC-5A are characterized by Equations 1 and 2. The exponent n is given values of 1, 2, 3, and 4 to find the highest linear correlation by Equation 2. The results are shown in Figure 1 by plotting a statistical correlation coefficient against n. The proposition $n = 3$ gives the best correlation, as Kawazoe et al. (5) have reported.

The characteristic curves obtained by setting $n = 3$ are shown in Figure 2 for ethylene by a plot of ln W against A. Similar results were obtained for other adsorbate gases of methane, ethane, propylene, and propane. However, the characteristic curves for *n*-butane and benzene are linear neither for $n = 3$ nor $n = 2$. The comparatively better correlation for *n*-butane was obtained for $n = 2$ as shown in Figure 3. The total pore volume W° is known from the intercept of the characteristic curve. The characteristic energy is estimated by reading value A at $W = 0.368\ W^\circ$ from the curve.

Results of the authors and Kawazoe et al. are listed in Table I. In principle, the total pore volume should be the same for all adsorbates. The differences in total pore volume found in Table I is attributed to difficulties in estimating liquid volume and hypothetical vapor pressure above the critical temperature and to the fact that adsorption occurs, not only in the micropores but also on the surface of macro and mesopores of MSC-5A. Kawazoe et al. reported that the characteristic energy for $n = 3$ approximately equals the heat of vaporization. That is proved for propane and propylene in this study. The calculated isotherms by Equations 1 and 2 using the values in Table I coincides well with the experimental ones having 4% standard deviation in relative adsorption amount.

Affinity coefficients calculated from the ratio of characteristic energy with ethane as a standard substance and from the liquid volume ratio at 30°C are shown in Table II where the average relative error between the former and the latter is about 10%.

The generalized characteristic curve for the systems of hydrocarbon–MSC-5A is shown in Figure 4. The solid line was determined by the least-squares method. In the high adsorption potential region where the temperature is high and the pressure is low, the data scatter a little because

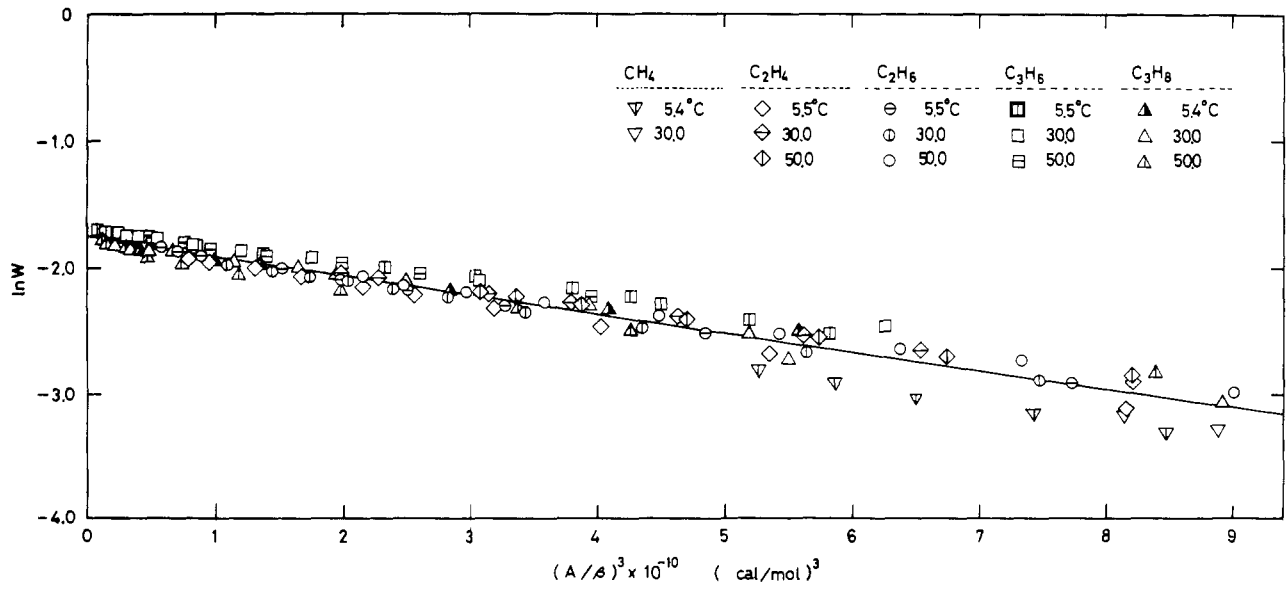

Figure 4. Generalized characteristic curve for hydrocarbon–MSC-5A systems

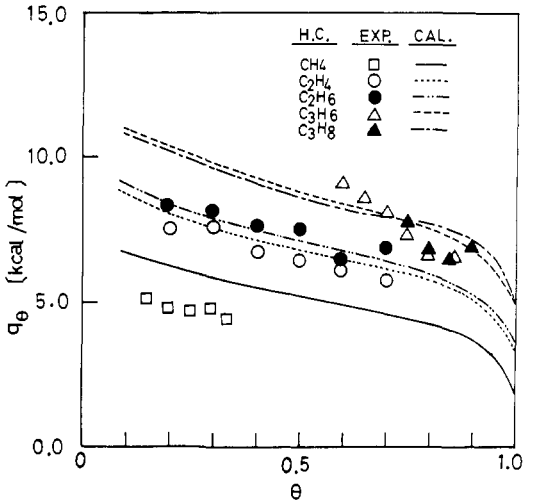

Figure 5. Differential heat of adsorption as function of adsorption ratio

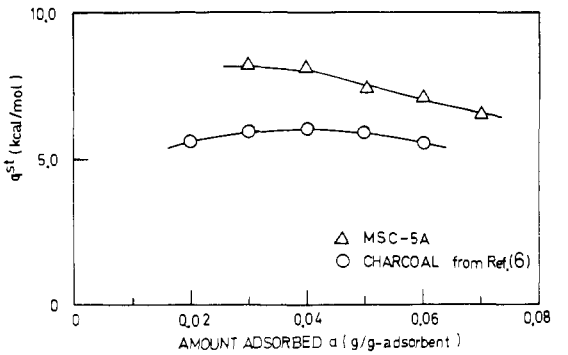

Figure 6. Isosteric heat of adsorption for ethane–MSC-5A and ethane–charcoal (BPL) systems

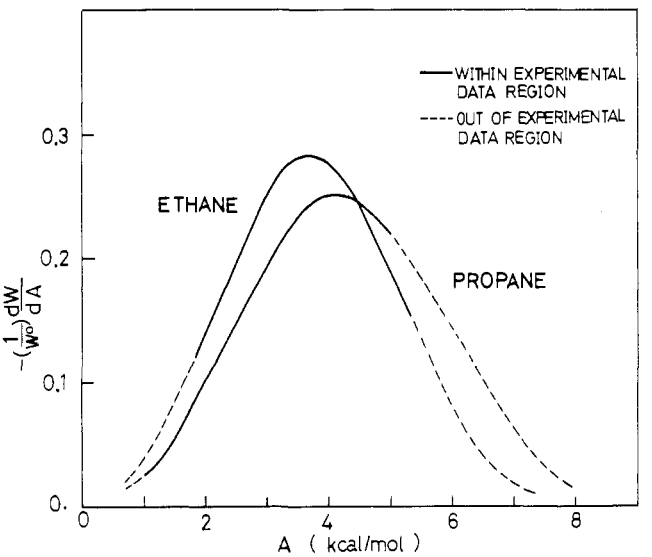

Figure 7. Distribution of adsorption potential for ethane–MSC-5A and propane–MSC-5A systems

Table III. Isosteric Heat of Adsorption for Hydrocarbon–MSC-5A Systems

Adsorbate	Amt adsorbed a, g/g-adsorbent	Isosteric heat of adsorption q^{st}, kcal/mol
Methane	0.0025	6.3
	0.0050	6.9
	0.0075	7.1
	0.0100	6.7
	0.0125	6.5
Ethylene	0.02	7.2
	0.03	7.8
	0.04	7.6
	0.05	8.0
Ethane	0.03	8.2
	0.04	8.1
	0.05	7.4
	0.06	7.2
Propylene	0.08	7.4
	0.09	8.1
Propane	0.07	8.5
	0.08	8.7

of the experimental error induced in a measurement of a small adsorption amount.

The differential heat of adsorption as a function of coverage is calculated by Equation 7, with the heat of vaporization taken from the "Handbook of Chemistry and Physics" (*4*). The experimental q_θ was obtained by Equation 6. Figure 5 shows the agreement between the calculated and experimental heats of adsorption for ethylene and ethane. The deviation observed in the figure for methane will be attributed to the error which occurred by the extrapolation of heat of vaporization into the supercritical region by about 200°. The isosteric heats of adsorption obtained from data are listed in Table III for methane, ethane, and propane.

The effect of micropores on heat of adsorption is estimated by comparing adsorptions of the same adsorbate on the adsorbents of identical chemical nature but of different surface structure. Comparison between isosteric heat of ethane on MSC-5A in this study and that on charcoal which is calculated from Laukhuf and Plank's data (*6*) in Figure 6 shows that adsorption heats in micropores are considerably higher.

The distribution of the adsorption potential of Equation 8 is figured for ethane–MSC-5A and propane–MSC-5A systems in Figure 7. The solid line represents the region where the experimental data of this work exist. The mean value of potential energies for ethane is smaller than that for propane, indicating higher interaction energies for the larger adsorbate molecules. From Equation 8, the curves are not symmetric—the right-hand side shoulders are higher than the left ones. To make clear the interpretation of the difference in shape of these two distribution curves, more experimental data in a wide potential range are required.

Acknowledgment

The authors are indebted to K. Kawazoe of Tokyo University for helpful advice.

Nomenclature

A = adsorption potential, cal/mol
a = adsorption amount, g/g-adsorbent
b = van der Waals constant, ml/mol
E = characteristic energy, cal/mol

ΔH = heat of vaporization, cal/mol
M = molecular weight
n = integer constant, Equation 2
P = pressure
q^{st} = isosteric heat of adsorption, cal/mol
q_θ = differential heat of adsorption at constant coverage, cal/mol
R = gas constant, 1.987 cal/mol/K
T = temperature, K
v = liquid molar volume, ml/mol
W = pore volume of adsorbent, ml/g-adsorbent, Equation 1
W° = total pore volume, ml/g-adsorbent

Greek Letters

β = affinity coefficient, E/E_o
ρ^* = adsorbed phase density, g/ml
ρ = liquid density, g/ml
θ = adsorption ratio

Subscripts

o = standard substance
b = normal boiling point
c = critical point
s = saturated state

Literature Cited

(1) Dubinin, M. M., "Adsorption-Desorption Phenomena," F. Ricca, Ed., p 3, Academic Press, New York, N.Y., 1972.
(2) Dubinin, M. M., *Chem. Rev.*, **60**, 235 (1960).
(3) Dubinin, M. M., "Chemistry and Physics of Carbon," Vol 2, p 51, Marcel Dekker, New York, N.Y., 1966.
(4) "Handbook of Chemistry and Physics," Chemical Rubber Publ., Cleveland, Ohio, 1971.
(5) Kawazoe, K., Astakhov, V. A., Kawai, T., Eguchi, Y., *Chem. Eng. Jap.*, **35**, 1006 (1971).
(6) Laukhuf, W. L. S., Plank, C. A., *J. Chem. Eng. Data*, **14**, 48 (1969).
(7) Nakahara, T., Hirata, M., Ohmori, T., *ibid.*, **19** (4), 310 (1974).
(8) Polanyi, M., *Verhandl. Deut. Phys. Ges.*, **16**, 1012 (1914).
(9) "Technical Data Book—Petroleum Refining," American Petroleum Institute, 1966.

Received for review June 18, 1974. Accepted October 23, 1974.

NEW COMPOUND SECTION

Synthesis of Benzo[a][1,4]benzothiazino[3,2-c]-phenothiazines and 5H-Benzo[a]phenothiazin-5-ones

Nand L. Agrawal and Ramji L. Mital[1]
Chemical Laboratories, University of Rajasthan, Jaipur 302004, India

A number of substituted benzo[a][1,4]benzothiazino[3,2-c]-phenothiazines and 5H-benzo[a]phenothiazin-5-ones are synthesized by the condensation reaction of 2,3-dichloro-1,4-naphthoquinone with substituted 2-aminothiophenols and their zinc salts, respectively. The lowering of C=O frequency in 5H-benzo[a]phenothiazin-5-ones is attributed to the ionic resonance effect.

The biological and industrial applications of phenothiazines and their derivatives have led to our interest in the synthesis of nuclear-substituted benzo[a]phenothiazines and their derivatives.

Van Allan and Reynolds (*10*), Akatsuka and Yoshinaga (*1*), and Reynolds et al. (*7*) have reported the synthesis of benzo[a][1,4]benzothiazino[3,2-c]-phenothiazine by the condensation of 2-aminothiophenol (ATPh) with 2,3-dichloro-1,4-naphthoquinone (I) and *N*-(1,4-dioxo-2-methoxynaphthyl-3)-pyridinium methosulfate. This reaction has been extended to a number of substituted 2-aminothiophenols (SATPH). It is quite interesting and surprising that under similar conditions the zinc salt of ATPh and I gave a different compound, i.e., 6-chloro-5H-benzo[a]phenothiazin-5-one. This unusual reaction seemed worthy of further investigation. 2-Amino-5-methoxy and ethoxy thiophenols were synthesized by a slightly modified method as reported earlier (*3–5*). The infrared data are also reported.

[1] To whom correspondence should be addressed.

Experimental

Ir spectra were recorded for KBr discs with a Beckman IR-4 spectrophotometer. 2-Amino-5-chloro- (*5*), 2-amino-5-bromo- (*5*), 2-amino-5-methyl- (*5*), 2-amino-5-fluoro- (*6*), 2-amino-3-bromo-5-methyl- (*9*), and 2-amino-3,5-dimethyl-benzenethiols (*9*) were prepared by the methods reported earlier. The purity of compounds was checked by tlc on silica gel G (Merck) in various nonaqueous solvent systems. All melting points are uncorrected.

5-Substituted (methoxy or ethoxy)-2-aminobenzenethiols. The hydrolysis of 2-amino-6-methoxy or ethoxy benzothiazoles (0.1 mole) was carried out with a small amount of potassium hydroxide (0.76 mole, 30% solution). This resulted in better yields (*5*) of 2-amino-5-methoxy or ethoxy benzenethiols. 2-Amino-5-methoxy-benzenethiol, yield 52%; mp 104°. 2-Amino-5-ethoxy-benzenethiol, yield 50%; mp 103°.